Journal of Materials Chemistry C

Accepted Manuscript

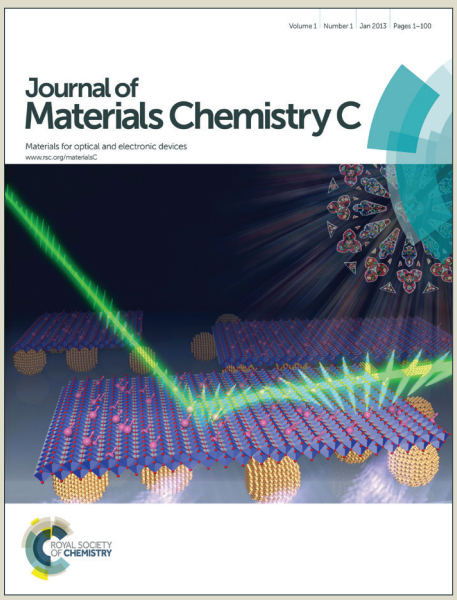

ROYAL SOCIETY OF CHEMISTRY

www.rsc.org/materialsC

Cite this: DOI: 10.1039/c0xx00000x

www.rsc.org/xxxxxx

ARTICLE TYPE

Highly Sensitive Explosive Sensing by "Aggregation Induced Phosphorescence" Active Cyclometalated Iridium(III) Complexes

Parvej Alam,[a] Gurpreet Kaur,[b] Vishal Kachwal,[a] Asish Gupta,[c] Angshuman Roy Chaudhury [b] and Inamur Rahaman Laskar*[a]

[a]Department of Chemistry, Birla Institute of Technology and Science, Pilani Campus, Pilani, Rajasthan, India, ir_laskar@bits-pilani.ac.in; [b]Department of Chemical Sciences, Indian Institute of Science Education and Research (IISER), Mohali, Sector 81, S. A. S. Nagar, Manauli PO, Mohali, Punjab, 140306, India, angshurc@iisermohali.ac.in; [c] Samtel Center for Display Technologies, IIT Kanpur, Kanpur, (U.P), India; ash@iitk.ac.in

Received (in XXX, XXX) Xth XXXXXXXXX 20XX, Accepted Xth XXXXXXXXX 20XX
DOI: 10.1039/b000000x

Two phosphorescent complexes, [Ir(o-CHOppy)$(PPh_3)_2$(H)Cl)] (1) and [Ir(ppy)$(PPh_3)_2$(H)Cl)] (2) exhibiting 'aggregation induced phosphorescent emission (AIPE)' property have been found to be very sensitive for the detection of picric acid (PA). The detection limit has been checked for PA and found the values of 264 nM and 65 nM with the complexes **1** and **2**, respectively.

Introduction

Today's society has a great threat from explosives through terrorist activities. The convenient way to detect such explosive materials poses a great challenge to the scientists to save human life and environments.[1] The nitro aromatics like trinitrotoluene (TNT), 2,4-dinitro phenol (2,4 DNP), picric acid (PA) etc. are well known explosive materials which are normally employed as tools in terrorist activities.[2] Further, out of these explosives, PA creates health hazard,[3] chronic diseases like cancer[4] and finally, it is used as powerful explosive similar to TNT.[5] In addition, PA is known as a notorious environmental polluting agent. Many detection techniques like Raman spectroscopy, cyclic voltammetry, gas chromatography, mass spectrometry, ion mobility spectrometry, electrochemical sensing, photoluminescence (PL) spectroscopy and many more have been used to detect such kind of explosives.[6] Among these reported techniques, PL based technique offers better sensitivity, shorter response time and economically viable.[7]

Similar electron affinity[8] of nitro aromatics appeals the scientific community to develop materials for highly sensitive and selective detection. As nitro aromatics by nature are electron deficient species, PL sensors developed with metal complexes/organic molecules worked on the principle of photo-induced electron transfer (PET) from donor to electron poor nitro aromatics (acceptor molecule) and subsequently results a PL quenching.[9] Thus, the linkage of electron rich moiety with the donor will facilitate the electron transfer to the acceptor molecule.[9a] Apart from being Lewis acidic electron acceptor nature, nitro phenolic aromatics (picric acid) functions as Bronsted acidic proton donor. In such case, the PL signal could be observed on shifting of maximum emission wavelength which was attributed to the supramolecular stacked nature of the ion pairs.[9b]

Iridium(III) based metal complexes have been mainly recognizable for their rich photo physical properties and colour tuning abilities.[10] The phosphorescence based Ir(III) complexes have better response time in the field of chemosensor in comparison to fluorescent materials.[11] 'Aggregation Caused Quenching (ACQ)' effect in the solid state creates difficulty in applying Ir(III) complexes in explosive detection. The main cause of very poor sensitivity and inefficiency of fluorophores in sensoric applications was resulted from the notorious ACQ effect[12]. There has a common strategy to minimize ACQ effect in emissive molecules is to integrate the bulky substituents with the fluorophores that will prevent the molecules to be closer in solid

phase[12d]. In 2001, an opposite phenomenon of ACQ was investigated and termed as 'aggregation induced emission (AIE)' effect.[13] In this case; a rotating unit (*e.g.*, phenyl) was attached with the fluorophore. It transformed the excited state molecule into non-luminescent in solution phase by dissipating the absorbed energy through rotation of this rotating units. The same excited state molecules exhibited strong luminescence in solid phase because of the locking of rotor with the neighbouring molecules.

AIE is a very simple process, while a tremendous problem solving phenomenon for various applications like sensors, bioimaging, lighting and organic light emitting diodes (OLEDs) etc.[14] In 2008, Q. Zhao *et al* reported the first 'aggregation induced phosphorescent emission (AIPE)' active Ir(III) phosphorescent complex.[15] The AIPE complexes showed the significant times of higher quantum efficiency in solid state in comparison to their solution state.[16] The development of new AIPE active Ir(III) based complexes keeps promise to solve many real problems for the mankind.

Till date, very few reports are found with AIPE active Ir(III) mediated complexes in detection of explosive materials. X.-G. Hou *et al* reported[9c] a maximum Stern–Volmer constant (K_{sv}), 5.28 x 10^4 M^{-1} for selective sensing of picric acid with Ir(III) complex while other two reports[9d,e] on Ir(III) are having K_{sv} values 7.42 x 10^4 M^{-1} and 3.56 x 10^3 M^{-1}, respectively for 2,4,6-trinitrotoluene (TNT) detection. These reports encourage the scientists to selective and sensitive detection of the explosive materials. Here, we have used two AIPE active Ir(III) phosphorescent complexes to selective and sensitive detection of nitroaromatics. The CHO functional group in **1** could be employed to integrate different functionalities with the AIPE entity. In addition, the electronic property of CHO shifts the maximum emission wavelength to red shift of **1** in comparison to the unsubstituted **2**. The bluish green emissive **2** has been employed successfully for selective and sensitive detection of PA while the **1** purposefully targeted only to sensitive detection of nitroaromatics. These probe molecules have shown a very high sensitivity in detection of picric acid with the observed values of 264 and 65 nM by **1** and **2**, respectively. Further, the maximum K_{sv} values of PA are observed 1.00 x 10^5 M^{-1} and 1.90 x 10^5 M^{-1} for **1** and **2**, respectively. These results making these complexes as super sensitive for explosive detection. In addition, the **2** has been successfully employed for selective detection of PA

EXPERIMENTAL SECTION

Materials: Iridium(III) chloride hydrate, 2-phenyl pyridine 4-(2-pyridyl)benzaldehyde, triphenylphosphine, 2-ethoxyethanol were purchased from Sigma Aldrich Chemical Company Ltd. Toluene, benzoic acid, 3,5 dinitro toluene, 1,3 dintro benzene, 2,5 dintro phenol, 2,4,6-trinitrophenol, and all spectroscopic grade solvents DCM, methanol etc. were procured from Merck Company.

Characterization: ^{1}H, ^{13}C and ^{31}P NMR spectra were recorded in 400 MHz Bruker spectrometer using $CDCl_3$ as solvent and tetramethylsilane (TMS, δ = 0 for ^{1}H and ^{13}C NMR) and phosphoric acid (H_3PO_4, δ = 0 for ^{31}P NMR) as internal standards. UV-VIS absorption spectra were recorded in Simadzu Spectrophotometer (model UV-1800 and 2550). The steady state photoluminescence spectra were recorded on Spectrofluorometer FLS920-s Edinburgh VARIO III. Particle sizes of the nano-aggregates were determined on a Malvern Zetasizer (MAL1040152). The solid state quantum yield of the thin film sample was measured using a calibrated integrating sphere in a Gemini spectrophotometer (Gemini 180). The photoluminescence (PL) spectra were recorded on a spectrofluoro photometer flouromax-4 (0406C-0809) and Simadzu (A40195003382SA). High-resolution MS (HRMS) were carried out with a (TOF MS ES$^+$ 1.38 eV) VG Analytical (70-S) spectrometer and Q-Tof micro mass spectrometer. Cyclic voltammetry (CV) measurements were recorded on a CHI Potentiostat Model 604E. The platinum wire, platinum and Ag/AgCl electrodes were used as counter, working and reference electrodes, respectively and the scan rate was maintained to 50 mVs^{-1}. The complex was dissolved in acetonitrile (10 mL) and 0.1 M lithium perchlorate ($LiClO_4$) (100 Mg) was added to the solution (used as a supporting electrolyte). The whole experiment was conducted under inert atmosphere.

Complex 1 ^{1}H NMR (400 MHz, $CDCl_3$) δ 9.15 (d, *J* = 5.5 Hz, 1H), 8.97 (s, 1H), 7.56 (d, *J* = 8.0 Hz, 1H), 7.49 – 7.30 (m, 15H), 7.15 (m, 18H), 6.81 (t, *J* = 6.0 Hz, 1H), 6.47 (s, 1H). δ -16.76 (t, *J* = 16.9 Hz, 1H); ^{13}C NMR (101 MHz, $CDCl_3$) δ 193.22, 150.69, 133.99, 133.99, 133.94, 133.88, 133.88, 131.86, 131.59, 131.31, 129.16, 129.16, 127.43, 127.38, 127.38, 127.33, 122.47, 121.40, 118.70, 117.65; ^{31}P NMR (162 MHz, $CDCl_3$) δ 7.93; ESI-HRMS calculated: ([M-Cl]$^+$): m/z, 900.2136, found: ([M-Cl]$^+$): m/z, 900.3271, yellow solid; Yield, 68.00 %.

Fabrication of thin-film on substrate for PL measurement

A 10^{-3} M solution of each of both complexes (in DCM) was

prepared. 2-3 drops of the solution were placed on a thin glass substrate (2 x 2 cm^2) and the solvent was allowed to evaporate slowly.

X-ray single crystal diffraction study

Single crystal X-ray diffraction data for the **1** was recorded on Bruker AXS KAPPA APEX-II CCD and Rigaku Mercury 375/M CD (XtaLAB mini) diffractometer respectively by using graphite Monochromated Mo – K_α radiation at 100.0(1) K by using Oxford cryosystem. The data sets collected on Bruker AXS KAPPA APEX-II Kappa were collected using Bruker APEX-II suit,[17] data reduction and integration were performed by SAINT V7.685A12[17] (Bruker AXS, 2009) and absorption corrections and scaling was done using SADABS V2008/112[17] (Bruker AXS). The data sets, which were collected on XtaLAB mini diffractometer, were processed with Rigaku Crystal Clear suite 2.0.[18] The crystal structures were solved by using SHELXS2013[19] and were refined using SHELXL2013 available within Olex2.[20] All the hydrogen atoms have been geometrically fixed and refined using the riding model except the hydride anion, co-ordinating with Ir, which has been located from the difference Fourier map and were refined isotropically. All the diagrams have been generated using Mercury 3.1.1.[21] Geometric calculations have been done using PARST [22] and PLATON.[23]

Results and discussion

The synthetic protocol for the parent **2** was reported earlier[24]. The **1** was synthesized by following the similar route as **2** (**Scheme 1**). Both complexes were characterized by ^1H, ^{13}C, ^{31}P NMR (**Fig. S1)** and SXRD (**Fig. 1**).

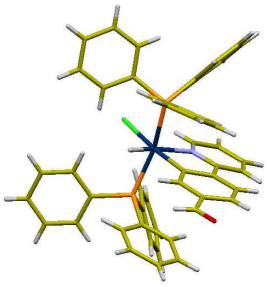

Fig. 1 ORTEP diagram for **1**, showing distorted octahedral geometry at the Ir site.

The NMR spectra of **1** shows few characteristic peaks such as ^1H NMR peak for CHO observed at δ= 8.97 ppm as singlet, hydride peak signal appeared at δ= −16.76 ppm as triplet (**Fig. S1a**) and the HRMS showing m/z= 900.3217 [M-Cl], as major fragment (**Fig. S1d**). The structural characterization of **2** is reported earlier.[24] The photophysical property along with AIPE property of **1** and **2**[25] has been investigated.

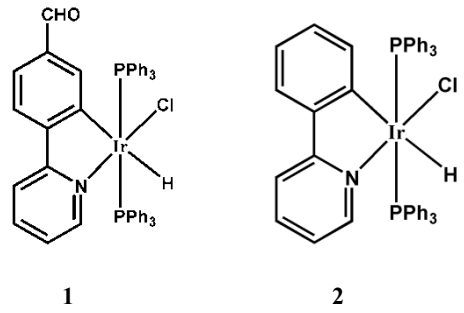

1 **2**

Scheme 1. Molecular structure of **1** and **2**

1 shows non luminescent nature in solution state with different organic solvents like dichloromethane (DCM), chloroform ($CHCl_3$), tetrahydrofuran (THF) and methanol (MeOH), but in solid state it emits strongly under UV-excitation at 365 nm.

To investigate the AIPE property in **1**, THF–water solvent mixture was used to perform the following experiment. The gradual enhancement of PL intensity was observed with increasing water fraction in THF-water mixture. With increasing water fraction (f_w), the soluble complex gets aggregated and that leads to the enhancement of PL intensity (**Fig. 2**).

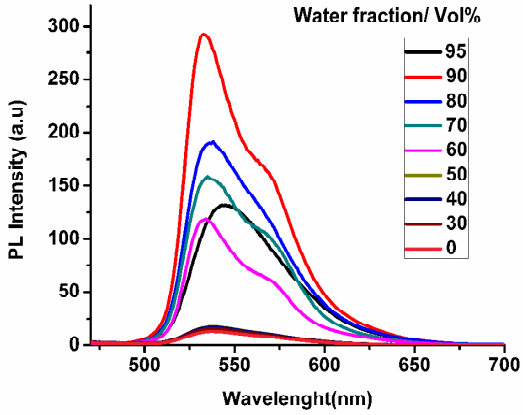

a

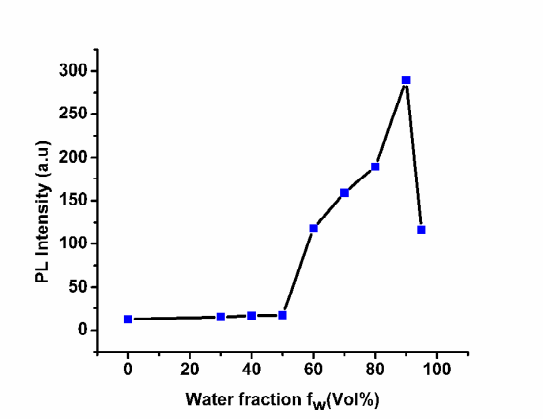

b

c

Fig. 2 (a) Emission spectra of **1** in THF/water mixtures; (b) intensity plot of intensity(I) values of **1** versus the compositions of the aqueous mixtures, Concentration: 1 x 10^{-5} M; (c) Photographs of **1** in THF/water mixtures with different water volume fractions (f_w) taken under UV illumination (λ_{exc}: 365 nm).

The reason behind of AIPE observation is due to the restricted intramolecular rotation (RIR) of phenyls in triphenylphosphines. The evidence of which is obtained from the packing diagram of **1** (**Fig. 3**). The packing diagram clearly showing C−H···π types several short contacts and these distances are within 2.85-2.88 Å. In these short contacts, phenyls in triphenylphosphines are involved. So, it leads to constraints in rotation of propeller shaped triphenyl phosphine in solid state, thus blocks the non-radiative pathways and generates AIPE activity in solid state. The average size of **1** in 90% water fractions (in THF/water) was measured by dynamic light scattering experiment and observed the size of the particle to ~291 nm (**Fig. S2**).

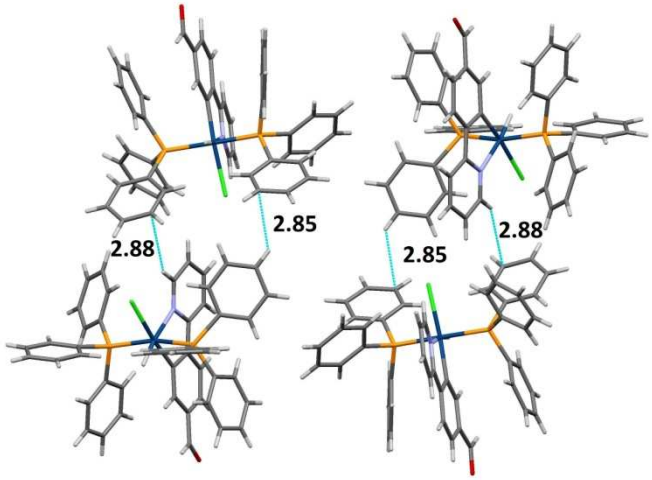

Fig. 3 Packing diagram for **1**; the unit cell contains four molecules and the interactions shown in blue lines (short contacts values were given in angstrom).

The quantum yield of **1** in DCM solution was obtained to 0.04%. The solid state quantum efficiency of **1** was measured with the help of integrating sphere to 22.60% and it was about 491 times higher than its solution quantum yield. The PL life time in pure THF solution and a solution with f_w= 90% (water/THF) of **1** was recorded and found to 2.5 ns and 4200 ns, respectively (**Fig. S3**). These findings support the observed remarkable AIPE property in **1**.

With considering the advantage of strong AIPE property of these complexes, we carried out the detection of different nitro aromatic along with few non-nitro aromatic compounds such as picric acid (PA), 2,4-dinitro phenol (2,4 DNP), 3,5-dinitro toluene (3,5 DNT), 1,3 dinitro benzene (1,3 DNB), nitro toluene (NT), benzoic acid (BA) and toluene (T) (benzoic acid and toluene are non-explosive). It was observed that the **1** resulted phosphorescent quenching after treatment of these nitro compounds (*vide infra*) with the phosphorescent complexes, separately. The maximum PL quenching was observed with PA where the detection limit was reached up to 264 nM (~98% quenching observed with 5 equivalents PA) (**Fig. 4**). On the other hand, **2** showed much better result in detection of PA where the detection limit was reached to 65 nM (~ 99% quenching observed with 5 equivalents PA) (**Fig. 5**).

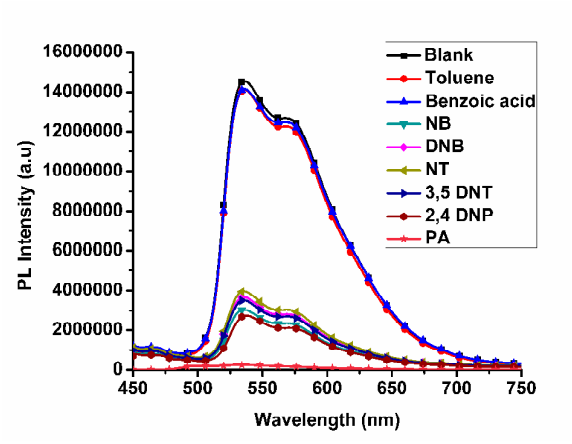

a

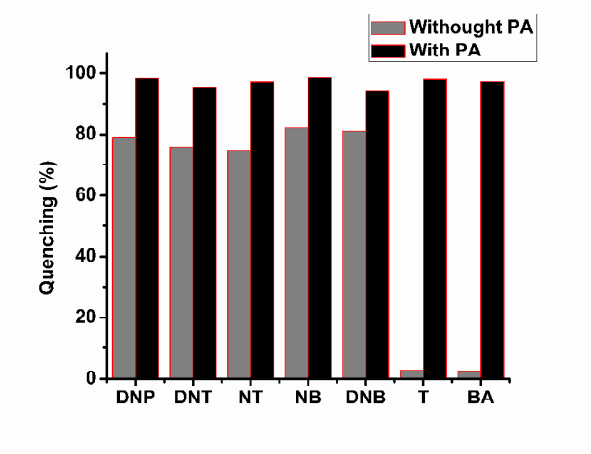

b

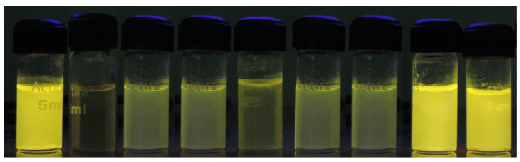

c

Fig. 4.(a) PL spectra of **1** with c =10^{-5} molL^{-1} at f_w = 90 % (in water/THF) upon the addition of 5 equivalents of different nitro based explosive /non explosive compounds (toluene, benzoic acid); (b) Column diagrams of the relative PL intensity of **1** with different explosive /non explosive compounds, at 535 nm. Grey bars represent the addition of various explosive /non explosive compounds to the complex **1** and black bars represents the subsequent addition of PA (5 equivalents) to the above solutions [**1** + explosive /non explosive compounds + PA]; (c) Image of **1** when dispersed at f_w = 90% with c = 10^{-5} molL^{-1}, with adding 5 equivalents of explosive /non explosive compounds, respectively; From left to right: (i) blank; (ii) PA; (iii) 3,5-DNT; (iv) NT; (v) 2,4-DNP; (vi) 1,3-DNB; (vii) NB; (viii) T; (ix) BA (under 356 nm UV lamp).

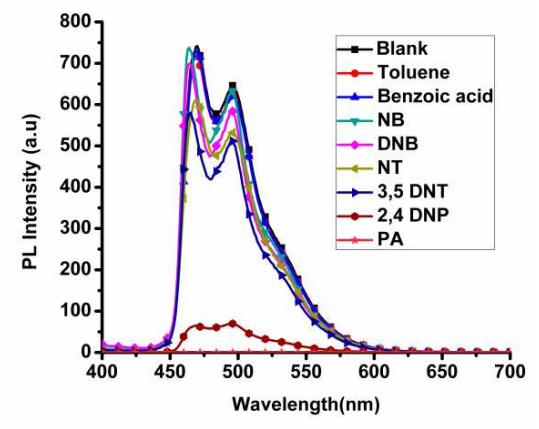

a

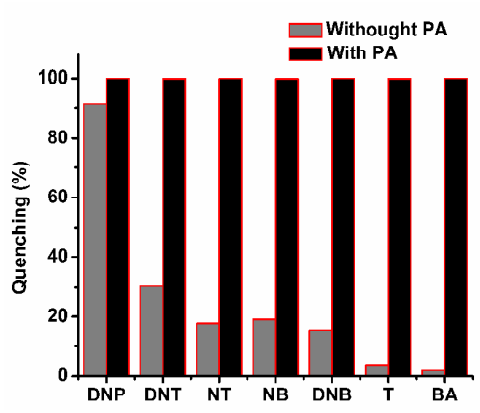

b

c

Fig. 5 (a) PL spectra of **2** with c =10^{-5} molL^{-1} at f_w = 90 % (in water/THF) upon the addition of 5 equivalents of different explosive /non explosive compounds; (b) Column diagrams of the relative PL intensity of **2** with different explosive /non explosive compounds, at 470 nm. Grey bars represent the addition of various explosive /non explosive compounds to the **2** and black bars represents the subsequent addition of PA (5 equivalents) to the above solutions [**2** + explosive /non explosive compounds + PA]; (c) Image of **2** when dispersed at f_w = 90% with c = 10^{-5} molL^{-1}, with addition of 5 equivalents of each explosive /non explosive compounds , respectively; from left to right: (i) blank; (ii) PA; (iii) 3,5-DNT; (iv) NT; (v) 2,4-DNP; (vi) 1,3-DNB; (vii) NB; (viii) T; (ix) BA

These results inspired us to check the sensitivity of PA with using both the complexes. The PL titration experiment of both the complexes was performed with increasing concentration of PA which shows a drastic drop in PL intensity in both cases. The Stern-Volmer (S-V) plot for both the complexes was non linear in nature and showing curves bending upward (**Fig. 6** & **7**). Thus, such a nature of S-V plot indicates the operation of static and dynamic quenching processes which demonstrate the quenching become more efficient with increasing concentration of PA. The quenching constants for both **1** and **2** have been calculated and found to 1.00 x 10^5 M^{-1} and 1.90 x 10^5 M^{-1}, respectively, which is much higher than the reported Ir(III) complexes[9].

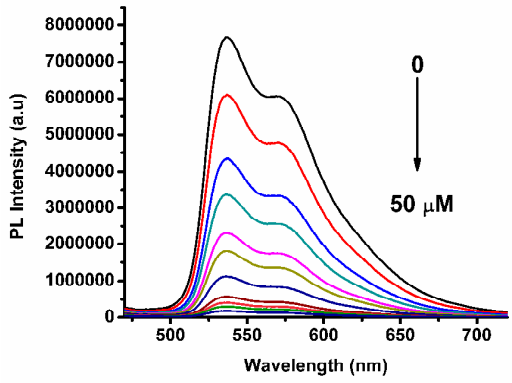

a

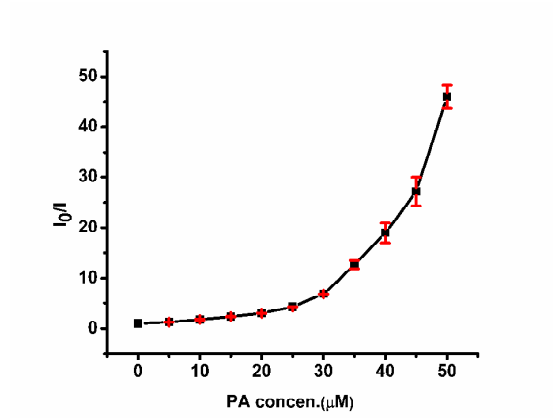

b

Fig. 6 PL spectra of **1** in THF–water (v/v = 1: 9) with different amounts of PA. (b) Corresponding Stern–Volmer plots of PA.

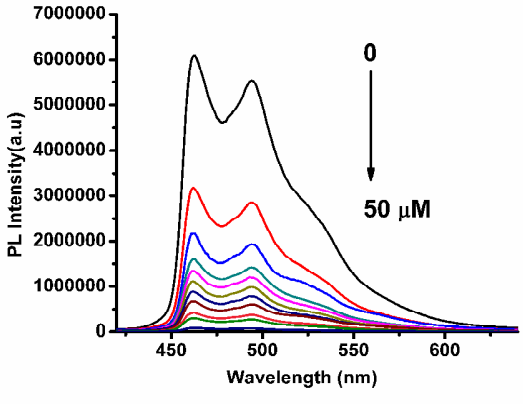

a

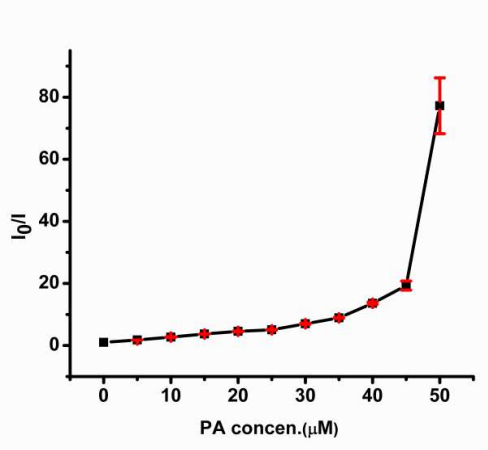

b

Fig. 7 PL spectra of **2** in THF–water (v/v = 1: 9) with different amounts of PA. (b) Corresponding Stern–Volmer plots of PA.

The HOMO and LUMO level of both the complexes were determined by cyclovoltametric measurements and band edge absorptions.The observed HOMO and LUMO energy levels are −5.58 eV and −2.89 eV for **1**, −5.47 eV and −2.48 eV for **2**, respectively (**Fig. S4**).

The mechanism of quenching for **1** was investigated. The nitro based explosives are highly electron deficient in nature because of the presence of strong electron withdrawing nitro functionality. The lowest unoccupied molecular orbital (LUMO) of nitro compounds were found to be lower in energy with respect to LUMO of **1**. The photo-induced electron transfer (PET)[18] is possible from LUMO of **1** to LUMO of NAs (nitro aromatics) [PA=−3.90 eV; DNT=−3.30 eV; NB=−3.35 eV], which resulted the PL quenching.[9]

The quenching and selective detection of PA by **2** may be

demonstrated either by PET or energy transfer (ET)[26] mechanism because these two mechanisms lead to quenching in the system. The energy transfer phenomenon may occur if the emission spectra of phosphors overlap with absorption band of the analytes,[9c] while the quenching caused PET is limited to the phosphors that has a direct interaction with the analytes. The ET mechanism may be one of the possible mechanisms for enhancing the detection sensitivity as well as selectivity. The absorbance spectra of nitro aromatics have been recorded in two systems, one is in THF and another is in THF-water mixture (1:9, v/v) (**Fig. S5**). The absorbance spectra of 2,4-DNP and PA show drastic change in THF-water medium in comparison to pure THF medium. The solution color becomes yellow in THF-water mixture which shows colorless in THF solution. Further, the absorption spectrum in THF-water system is red shifted with respect to the absorption spectrum in pure THF system **(Fig. 8)**. This change indicates the acidic nature of 2,4-DNP (pK_a = 4.10) and PA (pK_a = 0.40) in THF-water system.[27] PA can more easily dissociate in THF-water medium as compared to 2,4-DNP which is reflected from the lowing in pK_a value. This fact results relatively a larger extent of overlapping of absorption spectra of PA with the emission spectrum of **2 (Fig. 9)**.

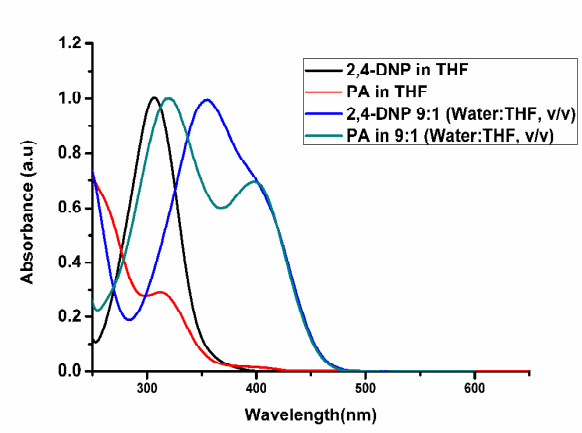

Fig. 8 Absorption spectra of 2, 4-DNP and PA in THF and (1:9, v/v) Water:THF mixture showing red shifted absorbance as compare to solutions in THF.

This might be the most plausible explanation for the observation of higher quenching efficiency of PA than 2, 4-DNP. Interestingly, the absorption spectra of 2,4-DNP and PA show a good overlapping with emission spectra of **2 (Fig. 9)**.

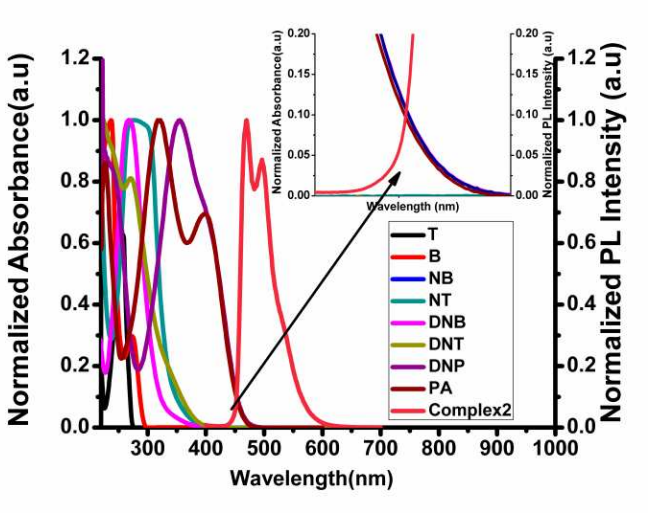

Fig. 9 Absorption spectra of different aromatic compounds and emission spectra of **2** in THF–water (v/v = 1: 9) mixtures. Inset: The spectral overlap between the emission of **2** and the absorption of 2,4 DNP and PA.

This larger extent of overlapping is undoubtedly responsible for efficient energy transfer which results quenching of light emission. In case of **1**, there was no overlapping observed between emission spectra of **1** and absorbance spectra of nitro aromatics under experiments **(Fig. S6)**.

The filter paper was soaked with the complex solutions (in DCM) shows clearly noticeable the quenching of emission color (**Fig. 10** & **S7**; λ_{exc} ~365nm).

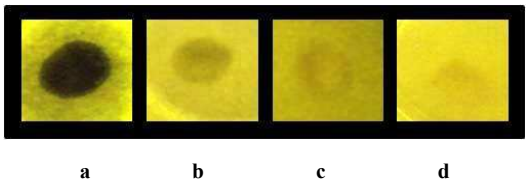

Fig. 10 Luminescent photographs of paper plates impregnated by **2** against different concentrations of PA (in M) (a) 10^{-3}; (b); 10^{-6}; (c) 10^{-9}; (d) 10^{-12}

Conclusions

In summary, two astounding AIPE Ir(III) complexes have been successfully employed for sensitive and selective detection of nitro-explosives. We have determined the Stern–Volmer quenching constant for both the complexes (K_{sv} =1.00 x 10^5 M^{-1} and 1.90 x 10^5 M^{-1} for **1** and **2**, respectively) and detection limit for PA is observed to 264 and 65 nM for the complexes **1** and **2**, respectively. The experimental observations support that both electron and energy transfer quenching mechanisms are responsible for the selective detection of PA by **2**. Filter paper based an easy way of detection of PA, a portable technique was developed.

Acknowledgements

We thank the 'Department of Science and Technology (DST), Govt. of India' under a project (No: SR/S1/IC-48/2009) and (No.: SB/S1/IC-13/2014) Council of Scientific and Industrial Research (CSIR) (No.01/2551/12/EMR-II), The 'UGC-SAP' and DST-FIST program for the chemistry department has been acknowledged for instrumental support. We, also thank IISER Mohali for the use of their single crystal X-ray diffraction and NMR research facilities.

Notes and references

Crystal data for complex 1: the CIF file have been submitted to the Cambridge Crystallographic Data Centre (CCDC) number is 1038913

1 (a) Y. Salinas, R. Martinez-Manez, M. D. Marcos, F. Sancenon, A. M. Costero, M. Parra and S. Gil, *Chem. Soc. Rev*., 2012, **41**, 1261-1296; (b) K. K. Kartha, S. S. Babu, S. Srinivasan and A. Ajayaghosh, *J. Am. Chem. Soc*., 2012, **134**, 4834-4841; (c) M. Kumar, V. Vij and V. Bhalla, *Langmuir*, 2012, **28**, 12417-12421.

2 M. E. Germain and M. J. Knapp, *Chem. Soc. Rev*., 2009, **38**, 2543 – 2555.

3 R. L. Woodfin, Trace Chemical Sensing of Explosives, John Wiley & Sons Inc., **2007**.

4 J. Shen, J. Zhang, Y. Zuo, L. Wang, X. Sun, J. Li, W. Han and R. He, *J. Hazard.Mater*., 2009, **163**, 1199-1206.

5 J. Akhavan, *Chemistry of Explosives, Royal Society of Chemistry*, 2nd edn**, 2004**; b) P. Cooper, *Explosive Engineering*, Wiley-VCH, **1996**, p.33.

6 (a) S. J. Toal and W. C. Trogler, *J. Mater. Chem*., 2006, **16**, 2871-2883; (b) A. Popov, H. Chen, O. N. Kharybin, E. N. Nikolaev and R. G. Cooks, *Chem.Commun*., 2005, 1953–1955.

7 (a) M. S. Meaney and V. L. McGuffin, *Anal. Bioanal. Chem*., 2008, **391**, 2557–2576; (b) T. K. Kim, J. H. Lee, D. Moon and H. R. Moon, *Inorg.Chem*., 2013, **52**, 589-595; (c) L. Li, S. Zhang, L. Xu, L. Han, Z. N. Chen and J. Luo, *Inorg. Chem*., 2013, **52**, 12323-12325; (d) Y. Bai, G. J. He, Y. G. Zhao, C. Y. Duan, D. B. Dang and Q. J. Meng, *Chem. Commun*., 2006, 1530-1532.

8 (a) S. Pramanik, C. Zheng, X. Zhang, T. J. Emge and J. Li, *J. Am. Chem. Soc*., **2011**, 133, 4153-4155; (b) B. Xu, X. Wu, H. Li, H. Tong and L. Wang, *Macromolecules*, 2011, **44**, 5089-5092.

9 (a) S. Shanmugaraju,S. A. Joshi and Partha Sarathi Mukherjee, *J. Mater. Chem*., 2011, **21**, 9130–9138; (b) M. Obulichetty and D. Saravanabharathi, *Spectrochim. Acta Part A: Mol. Biomol Spectrosc*., 2014, **118**, 861–866; (c) X.-G. Hou, Y. Wu, H.-T. Cao, H.-Z. Sun, H.-B. Li, G.-G. Shan and Z.-M.Su, *Chem. Commun.,*2014, **50**, 6031-6034; (d) K. S. Bejoymohandas, T. M. George, S. Bhattacharya, S. Natarajan and M. L. P. Reddy, *J. Mater. Chem. C*, 2014, **2**, 515–523; (e) T. Fei , K. Jiang and T. Zhang, *Sens. Actuators, B* , 2014, **199**, 148–153.

10 (a) C. Adachi, M. A. Baldo, M. E. Thompson and S. R. Forrest, *J. Appl. Phys*., 2001, **90**, 5048-5051; (b) S. Lamansky, P. Djurovich, D. Murphy, F. Abdel-Razzaq, H. E. Lee, C. Adachi, P. E. Burrows, S. R. Forrest and M. E. Thompson, *J. Am. Chem. Soc*., 2001, **123**, 4304-4312; (c) M. K. Nazeeruddin, R. Humphry-Baker, D. Berner, S. Rivier, L. Zuppiroli and M. Graetzel, *J. Am. Chem. Soc*., 2003, **125**, 8790; (d) M. A. Baldo, M. E. Thompson and S. R. Forrest, *Nature,* 2000, **403**, 750-753; (e) S. Reineke, F. Lindner, G. Schwartz, N. Seidler, K. Walzer, B. Lussem and K. Leo, *Nature*, 2009, **459**, 234-238; (f) J. Kido, M. Kimura and K. Nagai, *Science*, 1995, **267**, 1332-1334.

11 (a) P. Alam, G. Kaur, C. Climent, S. Pasha, D. Casanova, P. Alemany, A. R. Choudhury and I. R. Laskar, *Dalton Trans*., 2014, **43,** 16431–16440; (b) Q. Zhao, T. Y. Cao, F. Y. Li, X. H. Li, H. Jing, T. Yi and C. H. Huang, *Organometallics*, 2007, **26**, 2077–2081; (c) H. Yang, J.J. Qian, L. T. Li, Z. G. Zhou, D. R. Li, H. X. Wu and S. P. Yang, *Inorg.Chim. Acta*, 2010, **363**, 1755–1759; (d) F. Lu, M. Yamamura and T. Nabeshima, *Dalton Trans*., 2013, **42**, 12093–12100.

12 (a) M. Belletete, J. Bouchard, M. Leclerc and G. Durocher, *Macromolecules*, 2005, **38**, 880-887; (b) R. Jakubiak, C. J. Collison, W. C. Wan and L. Rothberg, *J. Phys. Chem. A*, 1999, **103**, 2394-2398; (c) M. Grell, D. D. C. Bradley, X. Long, T. Chamberlain, M. Inbasekaran, E. P. Woo and M. Soliman, *Acta Polym*.1998, **49,** 439-444;(d) S. Shanmugaraju, S.A. Joshi, and P. S. Mukherjee, *Inorg. Chem*., 2011, **50**, 11736–11745.

13 J. Luo, Z. Xie, J. W. Y. Lam, L. Cheng, H. Chen,C. Qiu, H. S. Kwok, X. Zhan, Y. Liu, D. Zhu and B. Z. Tang, *Chem.Commun*., 2001, 1740-1741.

14 (a) M. C. Zhao, M. Wang, H. J. Liu, D. S. Liu, G. X. Zhang, D. Q. Zhang and D. B. Zhu, *Langmuir*, 2009, **25**, 676-678; (b) W. X. Xue, G. X. Zhang, D. Q. Zhang and D. B. Zhu, *Org. Lett*., 2010, **12**, 2274-2277; (c) Y. Hong, J. W. Y. Lam and B. Z. Tang, *Chem. Soc. Rev*., 2011, **40**, 5361-5388; (d) D. Ding, K. Li, B. Liu and B. Z. Tang, *Acc. Chem. Res.*, 2013, **46**, 2441-2453; (e) W. Z. Yuan, Y.Gong, S. Chen, X. Y.Shen, J. W. Y. Lam, P. Lu, Y. Lu, Z.Wang, R. Hu, N. Xie, H. S. Kwok, Y. Zhang, J. Z.Sun and B.Z. Tang, *Chem. Mater*., 2012, **24**, 1518-1528.

15 Q. Zhao, L. Li, F. Li, M. Yu, Z. Liu, T. Yi and C. Huang, *Chem. Commun*., 2008, 685–687.

16 P. Alam, P. Das, C. Climentc, M. Karanam, D.Casanovac, A. R. Choudhury, P. Alemany, N. R. Jana and I. R. Laskar, *J. Mater. Chem* C, 2014, **2**, 5618-5628.

17 APEX2, SADABS and SAINT; Bruker AXS Inc.: Madison, Wisconsin, USA, 2008.

18 CrystalClear 2.0, Rigaku Corporation, Tokyo, Japan.

19 G. M. Sheldrick, *Acta Crystallogr. A.* 2008, **64**, 112.

20 O. V. Dolomanov, L. J.Bourhis, R. J.Gildea, J. A. K.Howard and H.Puschmann, *J. Appl. Cryst.* 2009, **42**, 339.

21 A. L. Spek, *Acta Crystallogr*. 2009, **D65**, 148.

22 M.Nardelli*, J. Appl. Cryst*. 1995, **28**, 569.

23 A. L. Spek, *Acta Crystallogr*. 2009**, D65**, 148

24 P. Alam, M. Karanam, A. Roy Choudhury and I. R. Laskar, *Dalton Trans.,* 2012, **41**, 9276-9279.

25 (a) V. Bhalla, A. Gupta and M. Kumar, *Org. Lett*., 2012, **14**, 3112-3115; (b) B. Roy, A. K. Bar, B. Gole and P. S. Mukherjee, *J. Org. Chem*., 2013, **78**, 1306-1310; (c) V. Bhalla, A. Gupta, M. Kumar, D. S. S. Rao and S. K. Prasad, *ACS Appl. Mater. Interfaces*, 2013, **5**, 672-679; (d) N. Venkatramaiah, S. Kumar and S. Patil, *Chem.Commun*., 2012, **48**, 5007-5009.

26 J. Wang, J. Mei, W. Yuan, P. Lu, A. Qin, J. Sun, Y. Ma and B. Z. Tang, *J. Mater. Chem*., 2011, **21**, 4056-4059.

27 N. Dey, S. K. Samanta and S. Bhattacharya, *ACS Appl. Mater. Interfaces*, 2013, **5**, 8394-8400.

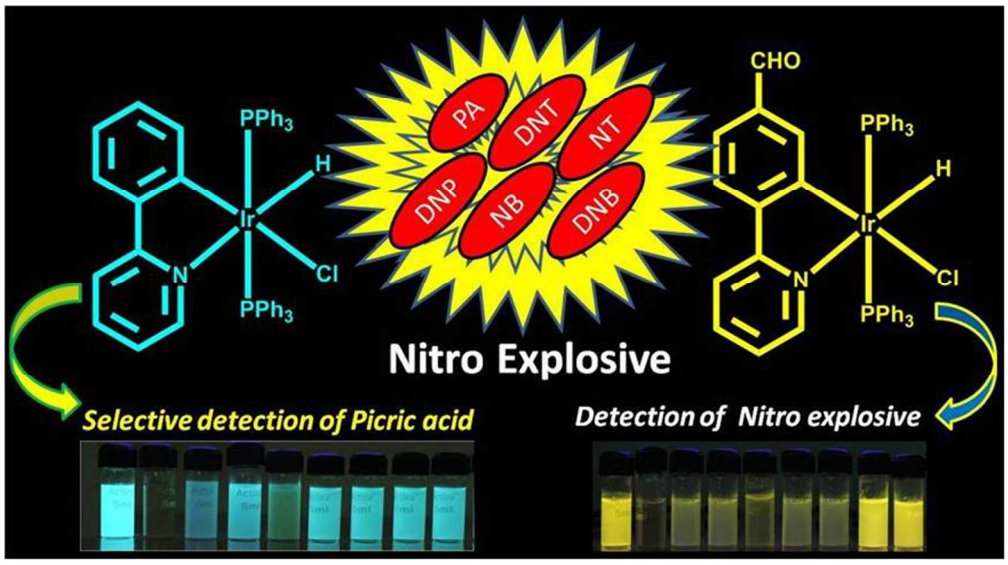

148x82mm (150 x 150 DPI)